

A Near-Term Quantum Algorithm for Computing Molecular and Materials Properties based on Recursive Variational Series Methods

Phillip W. K. Jensen,^{1,2,*} Peter D. Johnson,^{2,†} and Alexander A. Kunitsa^{2,‡}

¹*Chemical Physics Theory Group, Department of Chemistry,
University of Toronto, Toronto, Ontario M5G 1Z8, Canada*

²*Zapata Computing Inc., 100 Federal Street, Boston, MA 02110, USA*

(Dated: June 22, 2022)

Abstract

Determining properties of molecules and materials is one of the premier applications of quantum computing. A major question in the field is: how might we use imperfect near-term quantum computers to solve problems of practical value? We propose a quantum algorithm to estimate properties of molecules using near-term quantum devices. The method is a recursive variational series estimation method, where we expand an operator of interest in terms of Chebyshev polynomials, and evaluate each term in the expansion using a variational quantum algorithm. We test our method by computing the one-particle Green’s function in energy domain and the autocorrelation function in time domain, finding some advantages to this approach over existing methods.

1. INTRODUCTION

For quantum computers of the distant future, powerful quantum algorithms have been developed for solving problems in quantum chemistry and materials. These problems include estimating ground [1, 2] and excited state energies [3, 4], molecular gradients [5], and many others. However, implementing the quantum algorithms for problem instances of interest requires large-scale fault-tolerant quantum computers. What are the prospects for solving such problems with quantum computers before such large-scale devices are available? With the recent advances in quantum hardware, researchers have been investigating methods for using near-term quantum computers to solve problems of industry value. For the area of quantum chemistry and materials, much of this work has focused on the task of ground state energy estimation with the primary method being the variational quantum eigensolver (VQE) algorithm [6, 7]. Yet, for many problems of industrial value, properties beyond the ground state energy must be computed. To address this, the original VQE scheme was extended in two ways. First, it was combined with orthogonality constraints [8–10] and quantum subspace expansion (QSE) techniques [11, 12] to enable systematic exploration of the low-lying excited states. Second, finite-difference [13] and analytical derivative methods [14] were developed for the VQE energy functional to evaluate static molecular properties such as forces, vibrational frequencies, IR and Raman intensities, magnetic exchange and shielding constants, to name a few. The resource requirements for such calculations have not been studied in detail. All of them, however, rely on the standard VQE observable estimation routines and

* phillip.kastberg@gmail.com

† peter@zapatacomputing.com

‡ alex.kunitsa@zapatacomputing.com

are likely to suffer from the same measurement bottleneck [15]. Additionally, analytical derivative methods scale polynomially with the number of circuit parameters making them impractical for higher-order properties beyond relatively compact VQE ansatzes. At a more fundamental level, all of the VQE-based algorithms share a common limitation: they require explicit preparation of target wave functions (either exact or approximate) that are then used to evaluate physical observables. Although straightforward to implement, such approach is inefficient compared to other methods that can directly provide relevant quantities, such as correlation functions. More versatile quantum algorithms have been introduced in the context of linear response [16] and Green’s function [17, 18] formalism. Most of them rely on fault-tolerant computational subroutines [19–22] making their resource requirements prohibitive for implementation on noisy intermediate-scale quantum (NISQ) devices. This leaves open the question of whether efficient property estimation is feasible on the near-term quantum computers. Given that this is an important, though relatively underdeveloped area, it is valuable to explore novel approaches to solving these problems. Specifically, it is worthwhile to investigate alternative heuristic methods for estimating properties. Following the same design principles as their fault-tolerant counterparts, most of the known NISQ algorithms for property estimation were derived by replacing demanding computational subroutines with their near-term versions. For example, Variational Quantum Simulation [23] and Quantum Imaginary Time Evolution [24] were used to calculate correlation functions in real [25] and imaginary time [26–28], respectively. Similarly, variational linear system solvers were applied to response function calculations [29]. QSE and quantum Equation-of-Motion [12] methods were adapted for Green’s function evaluation [25, 30]. Most of these methods are fairly specific to the properties being estimated. Moreover, their performance is sensitive to the underlying assumptions and has not been thoroughly analyzed beyond small scale demonstrations on photonic and superconducting quantum devices [31–33]. With this motivation, our work explores the following question: How can we use near-term quantum computers to estimate molecular spectra and more general properties of approximate ground and excited states?

General dynamical properties can be expressed as spectral functions in energy (or frequency) domain. It is often sufficient to sketch a spectral function of interest to make predictions about certain properties. Viewed from this perspective, the problem can be tackled with classical approximation techniques such as kernel polynomial method [34] (KPM). KPM reconstructs spectral functions based on their moments in a suitable basis. For improved numerical stability they are commonly used in conjunction with Chebyshev expansion [35, 36]. This enables moment calcu-

lations via an iterative process which effectively applies a function of the Hamiltonian \hat{H} , $T_n(\hat{H})$, to an arbitrary initial state, where T_n is the n -th order Chebyshev polynomial of the first kind. This process is amenable to both classical and quantum computation. The main obstacle in the latter case is implementing the non-unitary operator $T_n(\hat{H})$ which can be accomplished, for example, with block-encodings [37]. Alternatively, one can circumvent the problem by switching to a Fourier basis, as shown in Ref. [38]. Lanczos recursion is closely related to KPM, but instead of using moment expansion it performs iterative construction of the continued fraction, representing a spectral function. Recently, it has been studied in the context of fault-tolerant [39] and near-term quantum computing as a tool for Green’s function calculations [40].

In this work, we introduce a flexible method for using low depth quantum circuits to estimate expectation values of general functions of a Hamiltonian with respect to an input state. It is inspired by KPM and has the same objective as the property estimation algorithm of Rall [37], while using far less circuit depth. In our method, a function of interest is approximated by a series expansion and we recursively train a parameterized circuit to approximate states proportional to the series terms applied to the input state. Accordingly, we refer to this method as *recursive variational series estimation* (RVSE). The method uses Hadamard tests to compute the overlaps between states output from short-depth quantum circuits, making this approach suitable for near-term quantum computation. We assess the performance of the method for two different applications with simulations that include statistical (sampling) noise, investigating the trade-off between the accuracy and error. Additionally, we model the buildup of error due to the recursive nature of the algorithm. Example applications of RVSE include estimating the spectrum for Green’s function methods and calculating autocorrelation functions.

The paper is structured as follows: In Section 2 we review the Chebyshev expansion method and some of its applications in quantum physics. Section 3 describes the details of RVSE. Computational tests of the algorithm are presented in Section 4 showcasing its performance for smooth and singular functions in the presence of sampling noise. We conclude with a discussion of open questions and future research directions in Section 5.

2. THE CHEBYSHEV METHOD

In this section we describe the mathematical technique that allows us to both control the accuracy of our property estimation as well as the number of iterations needed in the algorithm. The Chebyshev polynomials of the first kind are a class of orthogonal polynomials based on the

cosine function, $T_k(\omega) \equiv \cos(k \arccos \omega)$, such that any smooth function in the interval $\omega \in [-1, 1]$ can be expanded in a Chebyshev series:

$$f(\omega) = \sum_{k=0}^{\infty} c_k T_k(\omega) \quad (2.1)$$

where the expansion coefficients are given by

$$c_k = \frac{2 - \delta_{k0}}{\pi} \int_{-1}^1 \frac{f(\omega) T_k(\omega)}{\sqrt{1 - \omega^2}} d\omega. \quad (2.2)$$

The Chebyshev polynomials satisfy the following recurrence formula

$$T_k(\omega) = 2\omega T_{k-1}(\omega) - T_{k-2}(\omega), \quad (2.3)$$

such that only the last two polynomials are required at each step of recursion. For continuous functions $f(\omega)$, the expansion (2.1) converges uniformly on $[-1, 1]$ [41]. In practice, it can also be applied to singular functions in conjunction with regularization techniques described in [34]. The truncation of the infinite series in Eq. (2.1) leads to fluctuations — also known as Gibbs oscillations — near the points where the function is discontinuous [34]. This can be improved by using other kernels, e.g., the Jackson kernel, resulting in more smooth functions. In this work, we consider the simplest kernel: the Dirichlet kernel, but our method can be extended to other kernels. This can be further extended to operators, i.e., any operator function $\hat{f}(\hat{H})$ can be expressed in terms of the Chebyshev operators $\hat{T}_k(\hat{H})$ as long all of the eigenvalues of \hat{H} lie between $[-1, 1]$. If the condition does not hold the original operator needs to be re-scaled via a linear transformation:

$$\hat{H}_{\text{sc}} = (\hat{H} - H^+)/H^-, \quad (2.4)$$

where $H^\pm = (E_{\text{max}} \pm E_{\text{min}})/2$, and $E_{\text{min}}/E_{\text{max}}$ denote minimum and maximum eigenvalues of \hat{H} , respectively. We can loosen this restriction by chosen \tilde{H}_{max} and \tilde{H}_{min} such that $H_{\text{max}} < \tilde{H}_{\text{max}}$ and $H_{\text{min}} > \tilde{H}_{\text{min}}$ which ensure all the eigenvalues to lie between $(-1, 1)$.

Chebyshev expansion techniques found multiple applications in computational condensed matter physics [34] and quantum chemistry [42–46]. For example, it was shown by Tal-Ezer and Kolsloff [44] that expanding the time-evolution operator $\exp(-i\hat{H}t)$ in a K -term Chebyshev series converges exponentially for $K > t$ where t is the evolution time. Thus, long expansions

are not necessary which is computationally efficient in time. Other examples such as the imaginary time-evolution operator $\exp(-\tau\hat{H})$ exhibit an even faster convergence than the one found for the time-evolution operator [47], and Green’s functions have been expanded in the Chebyshev polynomials [42, 43, 45].

There are some advantages associated with the recursion method. Firstly, we can obtain approximate solutions at any step of the recursion. For example, the Lanczos algorithm [48], which has a similar recursion formula as in Eq. (2.3), is useful to compute the extrema eigenvalues from a Hamiltonian matrix. The extrema eigenvalues are resolved before the entire spectrum, and so one is not obligated to wait until the end of the calculation to estimate them. Secondly, recursive methods require only matrix-vector multiplication of the form $H\vec{c}$, and storing the Hamiltonian matrix is not necessary since it can be computed ‘on-the-fly’. For a sparse matrix, the number of non-zero elements scales as $\mathcal{O}(D)$, where D is the dimension of the matrix, and the calculation of a K -term Chebyshev expansion therefore requires $\mathcal{O}(KD)$ operations and time. For example, the molecular electronic Hamiltonian in the canonical Hartree-Fock spin orbital basis is sparse (see for instance [49]), and using the minimal operation-count method [50] and graphical representation of spin strings [51] yields an operation count identical to the computational theoretical limit. Thus, at first glance, it seems promising but since the dimension of the Hamiltonian matrix increases exponentially as a function of system size even matrix-vector multiplication for a sparse matrix becomes intractable. For example, a conventional binary computer can store $\sim 10^{10}$ amplitudes on a single core which correspond to a molecular system with only about 50 spin orbitals and 10 electrons all correlated. The dimensionality of the Hamiltonian matrix can however be reduced using approximate methods, but it has a cost of reducing the accuracy of the computed energies.

In this work, we explore recursive methods, specifically the Chebyshev method, on a digital quantum computer. The quantum algorithm proposed here overcomes the bottleneck of matrix-vector multiplication, but, as we will see, other problems arise such as sampling noise and circuit optimization. It is still an open question whether variational quantum algorithms alone can offer quantum advantage. For example, if the number of ansatz circuit parameters θ increases exponentially with system size, $\dim(\vec{\theta}) = \exp(\mathcal{O}(M))$ where M is number of basis functions, in order to reach the target accuracy then there is no advantage compared to the classical counterpart. A more interesting regime in which quantum advantage is viable is where only $\dim(\vec{\theta}) = \text{poly}(M)$ parameters are required to represent the target state with sufficient accuracy. In the following, we will assume all quantum states required to implement RVSE can be prepared efficiently, leaving a

more detailed exploration of this issue for future research.

3. RECURSIVE VARIATIONAL SERIES ESTIMATION METHOD

In this section we introduce the general recursive variational series estimation algorithm. The first step of the algorithm is to expand the target operator in the Chebyshev basis. Starting with an initial state $|\chi_0\rangle$, the action of the operator $\hat{F}(\hat{H})$ on the initial state can be evaluated by

$$\hat{F}(\hat{H}) |\chi_0\rangle \approx \sum_{k=0}^K c_k |\chi_k\rangle = \sum_{k=0}^K c_k \left(2\hat{H} |\chi_{k-1}\rangle - |\chi_{k-2}\rangle \right), \quad (3.1)$$

where $|\chi_k\rangle \equiv \hat{T}_k(\hat{H}) |\chi_0\rangle$. We can estimate the expectation value of the function $\hat{F}(\hat{H})$ as

$$\langle \chi_0 | \hat{F}(\hat{H}) | \chi_0 \rangle \approx \sum_{k=0}^K c_k \langle \chi_0 | \chi_k \rangle = \sum_{k=0}^K c_k \left(2 \langle \chi_0 | \hat{H} | \chi_{k-1} \rangle - \langle \chi_0 | \chi_{k-2} \rangle \right), \quad (3.2)$$

which requires the overlaps of the form $\langle \chi_0 | \hat{H} | \chi_{k-1} \rangle$ and $\langle \chi_0 | \chi_{k-2} \rangle$. In general, the Chebyshev operator $\hat{T}(\hat{H})$ is not unitary, and the resulting state $|\chi_k\rangle$ is therefore unnormalized. For that reason, we cannot directly prepare the Chebyshev states on a quantum computer. We can, however, represent a normalized state $|\tilde{\chi}_k\rangle = |\chi_k\rangle / \|\chi_k\|$ using a parametrized quantum circuit so that $|\tilde{\chi}_k\rangle = \hat{U}(\boldsymbol{\theta}_k) |0\rangle$ and $\boldsymbol{\theta}_k$ is a vector of real parameters. To prepare $|\tilde{\chi}_k\rangle$, we define an overlap between the true and normalized states as

$$\begin{aligned} F_k(\boldsymbol{\theta}) &= \langle 0 | \hat{U}^\dagger(\boldsymbol{\theta}) |\chi_k\rangle \\ &= 2 \langle 0 | \hat{U}^\dagger(\boldsymbol{\theta}) \hat{H} |\chi_{k-1}\rangle - \langle 0 | \hat{U}^\dagger(\boldsymbol{\theta}) |\chi_{k-2}\rangle \\ &= 2 \|\chi_{k-1}\| \langle 0 | \hat{U}^\dagger(\boldsymbol{\theta}) \hat{H} |\tilde{\chi}_{k-1}\rangle - \|\chi_{k-2}\| \langle 0 | \hat{U}^\dagger(\boldsymbol{\theta}) |\tilde{\chi}_{k-2}\rangle \\ &= 2 \|\chi_{k-1}\| \sum_{j=1}^L h_j \langle 0 | \hat{U}^\dagger(\boldsymbol{\theta}) \hat{P}_j \hat{U}(\boldsymbol{\theta}_{k-1}) | 0 \rangle - \|\chi_{k-2}\| \langle 0 | \hat{U}^\dagger(\boldsymbol{\theta}) \hat{U}(\boldsymbol{\theta}_{k-2}) | 0 \rangle, \end{aligned} \quad (3.3)$$

where the Hamiltonian is written in terms of Pauli strings $\hat{H} = \sum_{j=1}^L h_j \hat{P}_j$ with $h_j \in \mathbb{C}$ and \hat{P}_j is a Pauli string. A similarly strategy was proposed in Ref. [40] for preparing the Lanczos states on a quantum computer. We note that $|F_k(\boldsymbol{\theta})| \leq \|\chi_k\|$, and the maximum is achieved for the set of parameters $\boldsymbol{\theta}_k$ making $|\tilde{\chi}_k\rangle$ aligned with $|\chi_k\rangle$ such that $|F_k(\boldsymbol{\theta}_k)| = \|\chi_k\|$. The optimization is carried out by maximizing the absolute value of the overlap in (3.3). In an ideal situation the

optimized cost function results in the optimal angles $\boldsymbol{\theta}_k$, and the value of the cost function equals the normalizing constant $|||\chi_k\rangle||$. Lastly, we can compute each overlap in (3.2) as:

$$\langle\chi_0|\chi_k\rangle = |||\chi_0\rangle|| |||\chi_k\rangle|| \langle 0|\hat{U}^\dagger(\boldsymbol{\theta}_0)\hat{U}(\boldsymbol{\theta}_k)|0\rangle. \quad (3.4)$$

In practice, the optimization will be prone to errors due to e.g., sampling noise, decoherence, presence of local maxima, resulting in approximate angles and normalizing constants. Furthermore, recursive algorithms depend on previous steps in the algorithm (Eq. (2.3)) thus errors can propagate through the recursion and disrupt the computation. This is less of a problem for a classical computer since the matrix elements are evaluated with machine precision. We summarize the algorithm in Fig. 1.

We test the effect of sampling noise in Section 4 by adding errors from a normal distribution to the Chebyshev vector norms:

$$|||\chi_k\rangle|| \rightarrow |||\chi_k\rangle|| + \mathcal{N}_k(\mu = 0, \sigma^2), \quad (3.5)$$

where σ^2 is the variance and μ is the bias. The variance of the measured quantity and the number of measurements performed to estimate this quantity is related, and we can simulate the effect of sampling noise (but not device noise) by varying σ . The error in (3.5) will accumulate through the recursion, since the k 'th Chebyshev state depends on the previous two states. In this work, we do not account for the device noise, and assume the ansatz is expressive enough to reach the target states at each iteration, i.e., it is possible to find $\boldsymbol{\theta}_k$ such that $|\tilde{\chi}_k\rangle = \hat{U}(\boldsymbol{\theta}_k)|0\rangle$. In practice, however, this may not be the case due to limited circuit depth.

4. COMPUTATIONAL TESTS

4.1. The Green's Function

In this example, we consider the retarded one-particle Green's function (GF) at zero temperature defined as $G_{ij}^r(t) \equiv -i\theta(t) \langle\{\hat{c}_i(t), \hat{c}_j^\dagger(0)\}\rangle$, where $\theta(t)$ is the Heaviside step function, $\hat{c}_i(t) = e^{i\hat{H}t}\hat{c}_i e^{-i\hat{H}t}$ is the Heisenberg representation of the fermion annihilation operator \hat{c}_i , and $\langle\ldots\rangle = \langle E_0|\ldots|E_0\rangle$ denotes the expectation value with respect to the N -particle ground state of \hat{H} . It is assumed that we have already solved for the ground state, which itself is a highly non-trivial

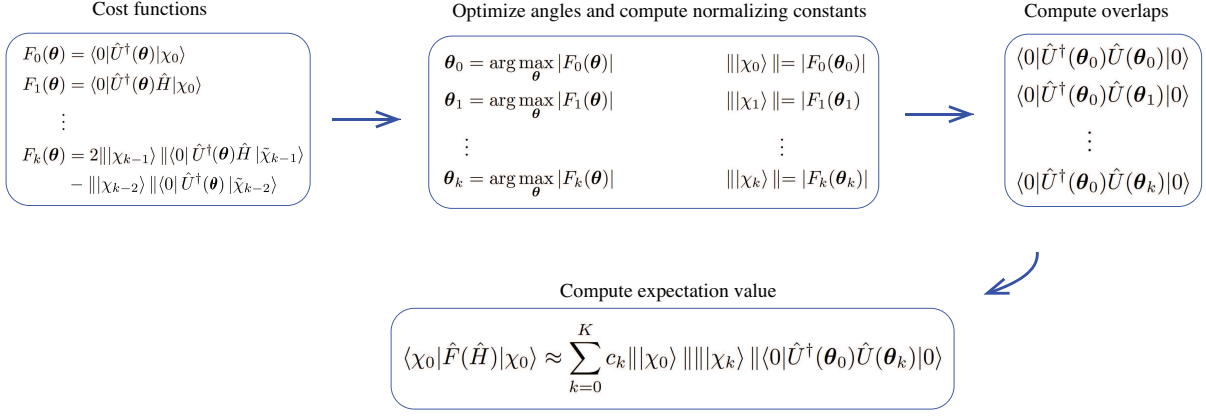


Figure 1. Schematic of the recursive variational series estimation method. The coefficients c_k are computed on a classical computer.

problem (see for instance [52–54]). The Green’s function is a central quantity in various fields, e.g., quantum transport theory [55], polarization propagator methods [56], photoemission spectroscopy, making it an important target for investigation. In the past couple of years several quantum algorithms have been proposed to compute GFs on a quantum computer [19, 22, 25, 30, 39, 40]. The method which is most similar to ours is the Lanczos recursion method [40], which variationally prepare the Lanczos states on a quantum computer, and compute the one-particle GF based on the continued fraction representation of the GF. We will compare the performance of the two methods later in this section.

If the Hamiltonian is time-independent, it is convenient to express the GF in the energy domain obtained by a Fourier transform:

$$G_{ij}^r(E) = \langle \Phi_i | \frac{1}{z^+ - \hat{H}} | \Phi^j \rangle - \langle \Phi^j | \frac{1}{z^- - \hat{H}} | \Phi_i \rangle, \quad (4.1)$$

where $z^\pm = \pm(E + i\eta) + E_0^{(N)}$ with $E_0^{(N)}$ as the ground state energy for the neutral system with N particles, and $|\Phi_i\rangle \equiv a_i |E_0\rangle$ ($|\Phi^j\rangle \equiv a_j^\dagger |E_0\rangle$) is the electron removal (attachment) state. We will focus on the spectral function, defined as the imaginary part of Eq. (4.1):

$$A_{ij}(E) \equiv -\frac{1}{\pi} \text{Im} G_{ij}^r(E) = -\frac{1}{\pi} \text{Im} \left(\langle \Phi_i | \frac{1}{z^+ - \hat{H}} | \Phi^j \rangle \right) + \frac{1}{\pi} \text{Im} \left(\langle \Phi^j | \frac{1}{z^- - \hat{H}} | \Phi_i \rangle \right). \quad (4.2)$$

The first and second term on the right hand side of (4.2) describe electron attachment and removal, respectively, and have poles at electron affinities (EA) and ionization potentials (IP). The width of the peaks is given by $\frac{1}{2}\eta$. The EA and IP, with respect to the ground state energy, are given

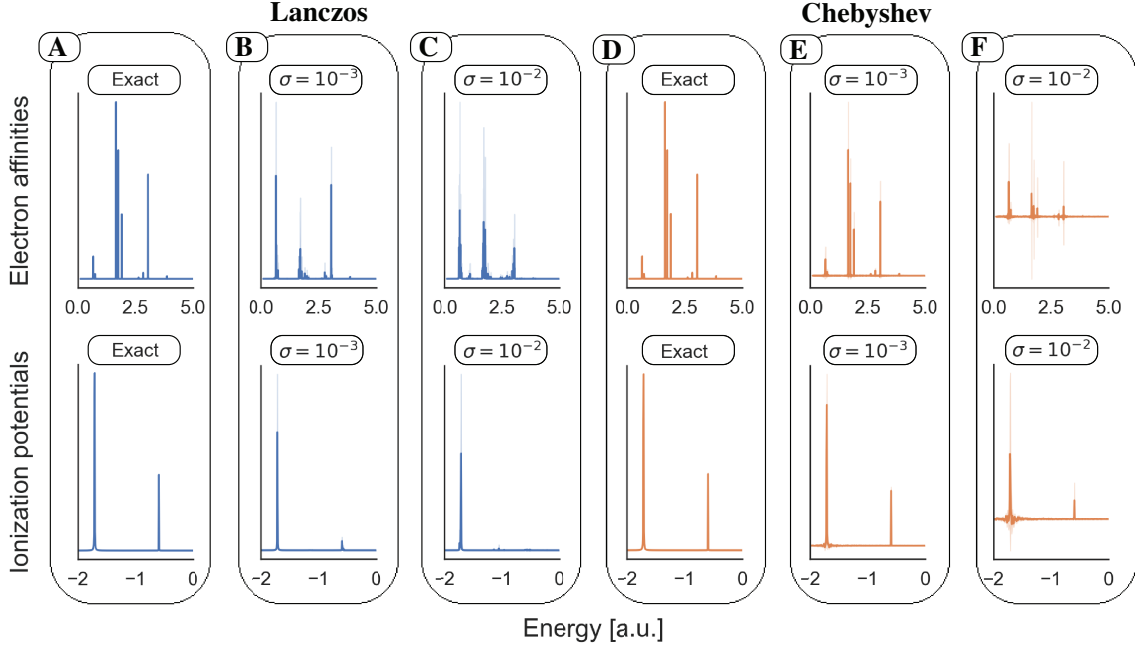


Figure 2. Electron affinities (EA) and ionization potentials (IP) for molecular hydrogen in the 6-31G basis. EA and IP are extracted from the first and second term in (4.2), respectively, for the diagonal element $A_{11}(E)$. Note, the plots show the negative values of EA and IP, and the energy for the Chebyshev method is rescaled back to the original spectrum to compare with the Lanczos method. The noisy simulations consist of 20 independent runs of the noisy spectral function, and we show the mean values with a confidence interval of 95 % ($\pm 1.96 \times$ standard deviation). We set the broadening parameter $\eta = 10^{-4}$, the number of terms in the Chebyshev expansion to $K = 40000$, and the convergence threshold for the Lanczos method to $\beta < 10^{-3}$. The molecular electronic Hamiltonian was generated using OpenFermion [57] and Psi4 [58].

by $EA_a = E_0^{(N)} - E_a^{(N+1)}$ and $IP_i = E_i^{(N-1)} - E_0^{(N)}$, respectively, and can be extracted from the spectral function. Note, the spectral function (4.2) has poles at the negative values of EA and IP. Thus, one can scan the energy axis in (4.2) looking for electron binding energies. In the limit $\eta \rightarrow 0^+$, the spectral function converges to a weighted sum of delta functions, $\lim_{\eta \rightarrow 0^+} A_{ij}(E) \rightarrow \sum_k a_k^{(ij)} \delta(E + E_0^{(N)} - E_k^{(N+1)}) + \sum_l b_l^{(ij)} \delta(E - E_0^{(N)} + E_l^{(N-1)})$.

We expand the expectation value of the Green's operator $(z - \hat{H})^{-1}$ with respect to an arbitrary state $|\chi_0\rangle$ in the Chebyshev basis as follows [59, 60]

$$\langle \chi_0 | \frac{1}{z - \hat{H}_{sc}} | \chi_0 \rangle = \frac{-i}{\sqrt{1 - z^2}} \sum_{k=0}^{\infty} (2 - \delta_{k0}) e^{-ik \arccos z} \langle \chi_0 | \hat{T}_k(\hat{H}_{sc}) | \chi_0 \rangle. \quad (4.3)$$

The overlaps $\langle \chi_0 | \hat{T}_k(\hat{H}_{sc}) | \chi_0 \rangle$ are then estimated on a quantum computer, as described in section 3. In this work, we simulate the RVSE algorithm on a classical computer in the presence of statistical (sampling) noise (Eq. (3.5)). Note, the expansion (4.3) does not decay as k increases, and truncation at finite k results in fluctuations, also known as Gibbs oscillations, near the points where the energy matches that of an eigenvalue. Consequently, even the last term contributes fully to the expansion making the spectral function a difficult target for the Chebyshev method. However, the fluctuation near the energy eigenvalues can be reduced using a different kernel which smoothing the function [34]. Further, the Chebyshev method requires a scaling of the Hamiltonian in (2.4) such that all of its eigenvalues lie between $[-1, 1]$. We will compare our method with the similar method in Ref. [40], which expresses the Hamiltonian in the Lanczos basis, resulting in the well-known continued fraction representation of the GF:

$$\langle \chi_0 | \frac{1}{z - \hat{H}} | \chi_0 \rangle = \frac{1}{z - \alpha_0 - \frac{\beta_1^2}{z - \alpha_1 - \dots}} \quad (4.4)$$

where the scalars α and β are the elements of the tridiagonal Hamiltonian matrix. For more information about the Lanczos method and the continued fraction representation of the GF, see for instance Ref. [60]. The Lanczos method can also compute off-diagonal elements of the GF by linear combinations of the diagonal elements in (4.4) [61]. In the following, we will test the performance of the two methods (4.3) and (4.4), specifically in the presence of sampling noise.

We test the methods by computing the diagonal element of the spectral function $A_{11}(E)$ for molecular hydrogen in the 6-31G basis at the equilibrium bond length 0.74144 Å, a system of 8 spin orbitals — one of the simplest, still non-trivial, molecular systems. We set the initial state in the recursion to $|\chi_0\rangle = |\Phi_1\rangle = \hat{a}_1 |E_0\rangle$ and $|\chi_0\rangle \equiv |\Phi^1\rangle = \hat{a}_1^\dagger |E_0\rangle$ for ionization potentials and electron affinities, respectively. The molecular orbital index runs from $0, \dots, 7$. Note, adding or removing an electron result in a non-normalized state. In Fig. 2, we show EA and IP extracted from the first and last term in (4.2), respectively, using the Chebyshev method (4.3) and Lanczos method (4.4). Fig. 2 (A) and (D) show the exact (noiseless) case where only truncation error is presented in the algorithm, and the peaks correspond to EA and IP energies. The magnitude of the spectral function is omitted, since the location of the peaks are important, not the magnitude, if the target is to extract charged excitations. We observe that the spectra produced by Lanczos and Chebyshev are almost identical, but they differ in run-time. The Lanczos method converges after a few iterations and is therefore particular useful to approximate these type of functions. The Chebyshev method is known to perform poorly near singularities/sharp peaks, and would

require many terms in the expansion to reduce the fluctuations near the peaks. In the simulations a total of $K = 40000$ terms are used in the expansion in order to obtain a smooth function, and we can distinguish the tiny peaks corresponding to eigenvalues from background oscillation in the spectrum. Although the Lanczos method converges fast its run-time is still larger than the Chebyshev method using the protocol in Ref. [40]. The reason is that the off-diagonal element β is expensive to evaluate on a quantum computer. We refer the reader to Appendix A for a detailed analysis of the run-time estimate for the two methods.

In the remaining plots (B, C, E and F), we test the effect of sampling noise. We simulate sampling noise by adding errors from a normal distribution to the normalizing constants for the Chebyshev method, see Eq. (3.5), and similar for the Lanczos method to the matrix elements: $\alpha_k \rightarrow \alpha_k + \mathcal{N}_k(\mu = 0, \sigma^2)$ and $\beta_k \rightarrow \beta_k + \mathcal{N}_k(\mu = 0, \sigma^2)$, where σ^2 is the variance and μ is the bias. The variance of the measured quantity and the number of measurements performed to estimate this quantity is related, see Eqs. (A.5) and (A.7) in Appendix A. Furthermore, in order to make a fair comparison between the two methods with respect to run-time, we set the number of terms in the Chebyshev expansion to $K = 40000$, as described in Appendix A, which is also large enough to reduce the background oscillation. We observe for the Lanczos method “spurious” eigenvalues, which appear randomly in the energy spectrum and do not correspond to actual eigenvalues. This is particularly the case for the EA simulations. For the IP simulations we observe only two peaks in the spectrum, and the spurious-peak phenomenon becomes less of a problem. This is not related to the IP calculations, but the spectrum being much less dense than the EA simulations. This phenomenon can be observed more clearly in Fig. 3 which show the mean absolute error for Figs. 2 (B) and (E). For example, in Fig. 3 (B) we clearly observe an increasing error in the middle of the spectrum for the Lanczos method corresponding to spurious eigenvalues. The spurious-peak phenomenon for the Lanczos method is a well-known problem in classical computing, mainly due to round-off errors. Round-off errors even at machine precision can have an effect for recursive methods, especially for the Lanczos recursion which has a similar recursion formula as in Eq. (2.3), where it was shown that the loss of global orthogonality among the Lanczos vectors arise from round-off errors causing the spurious eigenvalues [62–66]. It seems that sampling noise amplifies this effect. For the Chebyshev method, the peaks did not move significantly, i.e., they correspond to actual charged excitations. In the case the sampling error gets too large ($\sigma = 10^{-2}$), it becomes hard to distinguish the peaks from the background resulting in the spectral information being lost.

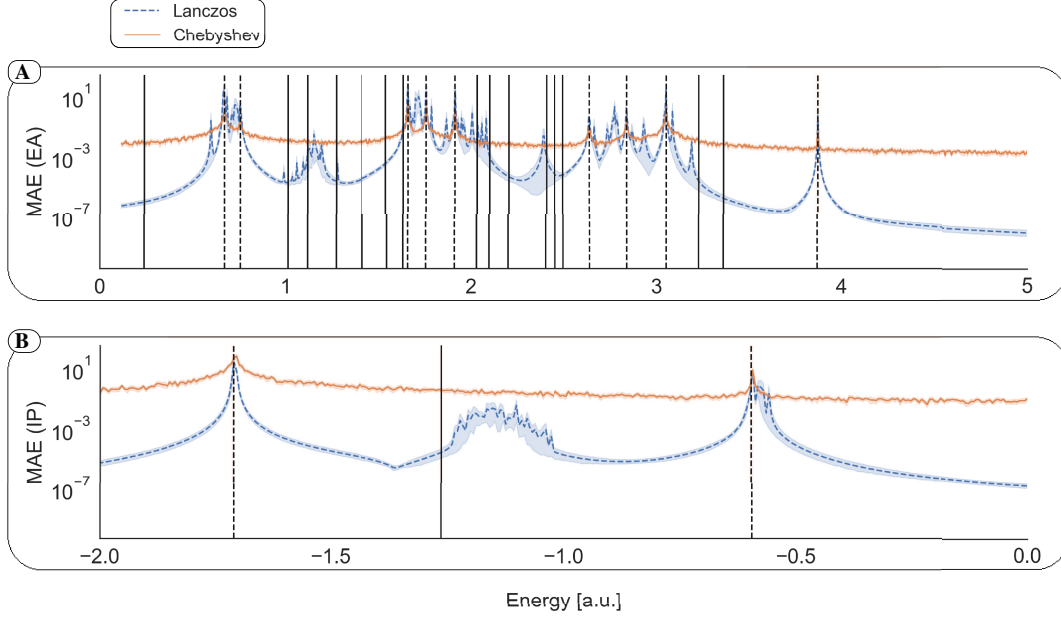


Figure 3. The mean absolute error (MAE) for the noisy electron affinities (EA) and ionization potentials (IP) for the simulations in Fig. 2 (B) and (E), i.e., $\sigma = 10^{-3}$. The dashed vertical lines correspond to the observable peaks in Fig. 2 (A) and (D), and the solid vertical lines correspond to the non-observable charged excitations, i.e., having a negligible overlap with the initial state. The simulations consist of 20 independent runs of the noisy spectral function, and we show the MAE values with a confidence interval of 95 % ($\pm 1.96 \times$ standard deviation).

4.2. The Auto-Correlation Function

The Chebyshev expansion of the time-evolution operator were worked out by Tal-Ezer and Kosloff [44]:

$$e^{-i\hat{H}_{sc}t} \approx \sum_{k=0}^K (2 - \delta_{k0}) (-i)^k J_k(t) \hat{T}_k(\hat{H}_{sc}), \quad (4.5)$$

where J_k is the Bessel function of the first kind, and the truncation error can be bounded as [67, 68]

$$\epsilon = \|\hat{U}_K - \hat{U}_\infty\| \leq \sum_{k=K+1}^{\infty} 2|J_k(t)| \leq \frac{4t^{K+1}}{2^{K+1}K!} \quad (4.6)$$

where \hat{U}_∞ is the exact unitary operation. The error dramatically decreases for $K > t$, and only a small number of extra terms are needed after reaching t . The auto-correlation function can then be approximated as

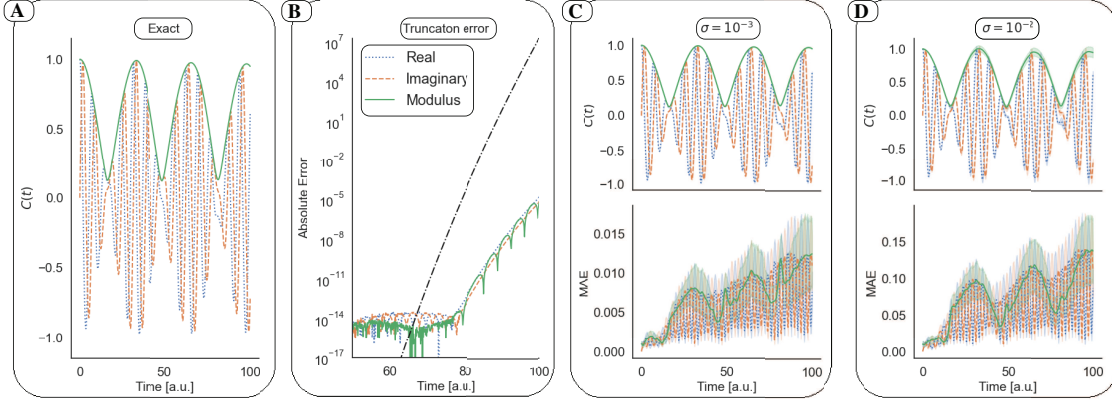


Figure 4. Auto-correlation function $C(t)$ in the time domain for molecular hydrogen in the 6-31G basis. The real, imaginary and module of the correlation function are represented by dots (blue), dashed (orange) and solid (green) lines, respectively. The dashdot (black) line in Fig. (B) shows the upper bound truncation error given in Eq. (4.6) with $K = 120$. The MAE (mean absolute error) simulations consist of 20 independent runs of the noisy auto-correlation function with $K = 120$, and a confidence interval of 95 % ($\pm 1.96 \times$ standard deviation). The molecular electronic Hamiltonian was generated using OpenFermion [57] and Psi4 [58].

$$C(t) \equiv \langle \Psi | \Psi(t) \rangle \approx \sum_{k=0}^K (2 - \delta_{k0}) (-i)^k J_k(t) \langle \Psi | \hat{T}_k(\hat{H}_{sc}) | \Psi \rangle. \quad (4.7)$$

Compared to the spectral function in the previous section, the auto-correlation function converges much faster. It is known that the Chebyshev expansion leads to relatively poor convergence at the discontinuities or singularities due to increasing fluctuations, and the spectral function is a weighted sum of sharp peaks. Hence it requires many terms in the expansion. We used 40000 terms for the molecular hydrogen. The auto-correlation function, on the other hand, is continuous and does not have discontinuities or singularities but exhibits a wave-like behavior. The Chebyshev polynomials seem to be a ‘natural’ choice of basis for these type of functions. The Lanczos basis on the other hand is better for representing the spectral function since only a few iterations were needed for convergence for molecular hydrogen. Lanczos comes with an added benefit of the continued fraction expansion that already has singularities built in (4.4), even for a finite level of truncation. With Chebyshev we don’t have this luxury.

We test our method by computing the auto-correlation function in (4.7) for molecular hydrogen

in the 6-31G basis, a system of 8 spin orbitals, at equilibrium bond length 0.74144 Å. We set the initial state to $|\chi_0\rangle = |\Psi\rangle = \frac{1}{\sqrt{2}}(|\phi_0\phi_1\rangle + |\phi_2\phi_3\rangle)$, where $|\phi_i\phi_j\rangle$ indicates the spin orbitals i and j are occupied. In Fig. 4 (A), the exact auto-correlation function is shown; $C(t) = \sum_n |\langle E_n | \Psi \rangle|^2 e^{-iE_n t}$ expanded in the energy eigenbasis of the Hamiltonian, and we performed an exact diagonalization of the Hamiltonian. The auto-correlation function is a wave function consisting of a mix of eigenstates each contributing a different period of $2\pi/|E_n|$. In Fig. 4 (B), the auto-correlation function is approximated with a 120-term Chebyshev expansion, and we show the truncation error for the real, imaginary and modulus part of the auto-correlation function. An interesting observing is the extremely loose bound in (4.6) by a difference of more than 10 orders of magnitude compared to the exact truncation error. As expected, the truncation error increases for increasing evolution time, which can be suppressed by increasing the number of terms in the expansion. If restricted to 120 terms, the auto-correlation function can be simulated with machine precision up to $t \sim 80$ atomic time. Note, for the spectral function in the previous section, we required 40000 terms in the expansion to observe all peaks (due to small overlap with the initial state), making the spectral function significantly more computationally expensive than the auto-correlation function.

We tested our method in the presence of sampling noise by adding errors from a normal distribution, see Eq. (3.5). That is, the auto-correlation function in Figs. 4 (C) and (D) is computed using the RVSE method in section 3. We wanted to investigate how the error builds up through the recursion. Firstly, we observe that the main contribution to the overall error comes from the sampling noise, not the truncation error which is insignificant compared to sampling noise. Secondly, increasing the sampling noise by a factor of 10, the error increases approximately with a factor of 10 for each time step. Thirdly, the error increases with increasing evolution time, as expected, since the error accumulates through the recursion.

5. CONCLUSION AND OUTLOOK

RVSE is a mathematical framework for estimating expectation values of general operators. Its key component is a series expansion of a target operator in the Chebyshev polynomial basis which can be implemented variationally by introducing an ansatz for each term. RVSE is therefore inspired by the Kernel Polynomial Method used to compute spectral functions on classical computers [34], but is applicable in a more general context. Here, we focused on the problem of evaluating expectation values of operators represented as functions of the Hamiltonian. Specifically, we tested RVSE for Hamiltonian simulation and one-particle Green's function calculations, both of which

are promising applications of near-term quantum computers. Without performing a detailed comparison with the state-of-the-art algorithms (except for the closely related Lanczos method [40]), we focused on assessing the noise resilience of RVSE and its resource efficiency through numerical simulations. Our implementation benefits from recursive properties of Chebyshev polynomials to avoid estimating increasingly high powers of the Hamiltonian operator $\langle \hat{H}^k \rangle$. This keeps the number of measurements approximately constant at each step of recursion, but introduces interdependence between the consecutive terms in the series allowing sampling noise amplification. The latter presents a difficulty when applying RVSE to estimation problems that require long expansions, such as the spectral function calculation. Yet, compared to the Lanczos method, recently proposed for the same purpose [40], our algorithm is not susceptible to the occurrence of spurious peaks and faithfully reproduces the overall shape of spectral function for the model example of H_2 molecule. Using the auto-correlation function as another example, we studied the interplay of the series truncation and sampling noise accrued while evaluating it. The Chebyshev basis is known to be efficient for representing the time evolution operator and has been previously used to derive optimized Hamiltonian simulation algorithms [68]. RVSE adopts a similar approach offering an alternative to existing near-term methods such as VQS [8] and related techniques [23, 69]. Depending on simulation time, only a few terms of Chebyshev expansion are required to accurately simulate electron dynamics. In particular, for the H_2 molecule we truncated the series at 120 terms to be contrasted to a much larger value of 40000 for the spectral function calculation. Due to the low depth of recursion used to evaluate the propagator it shows less sensitivity to sampling noise compared to the spectral function. Given the constraints of modern quantum hardware we expect RVSE to be practical only for certain types of property estimation problems. Our numerical studies show that controlling the convergence rate (i.e. the number of terms) of the Chebyshev series is crucial for minimizing the measurement cost of RVSE. Therefore, establishing the limits imposed by noise amplification on the depth of recursion is an important direction of future work. We analyzed the performance of the algorithm in the presence of sampling noise assuming that the expectation values of the individual terms in Chebyshev series can be computed without systematic error. This implies that at k -th step of recursion the Chebyshev vector $|\chi_k\rangle$ can be prepared by a compact and expressive ansatz. We anticipate the number of parameters in such an ansatz to increase with k making cost function optimization increasingly challenging due to the notorious barren plateau phenomenon [70]. To some extent it can be mitigated by adaptive ansatz construction [71] which appears to be well suited for RVSE. In experiments on noisy quan-

tum devices systematic errors are unavoidable due to the presence of decoherence effects. Similar to the sampling noise hardware errors can get amplified throughout recursion deteriorating the accuracy of the higher order terms. We leave a more detailed exploration of this effect for future work. Another direction is to explore the performance of RSVE applied to expectation values of other functions of the Hamiltonian. One interesting example is the threshold function from Dong, Tong, and Lin [72], which is used for ground state energy estimation. Imaginary time evolution is another promising application for RVSE [47]. Finally, RVSE is fully compatible with the KPM framework in that it is not limited to the Dirichlet kernel adopted in this work. Furthermore, it can be incorporated into hybrid KPM methods [73] and used in conjunction with embedding techniques [74] to study spectral properties of condensed matter systems. As such we hope it opens new avenues of research directed at identifying quantum computing applications holding a promise for industrially relevant quantum advantage.

6. ACKNOWLEDGEMENT

We thank Chong Sun, Max Radin, and Jerome Gonthier for detailed feedback on the manuscript. We thank Lasse Bjørn Kristensen for helpful discussions. P.W.K.J acknowledges support by Augustinus Fonden, Knud Højgaards Fonden, and Viet-Jacobsens Fonden.

Appendix A: Runtime Estimation for the Lanczos and the Chebyshev Methods

For the Lanczos method, we follow the work in Ref. [40], a protocol to compute the matrix elements α and β of the tridiagonal Hamiltonian matrix, which can then be used to compute the Green's function in Eq. (4.4). As opposed to the Chebyshev states, the Lanczos states generated through the recursion are normalized, and it is possible to prepare them directly on a quantum computer. In Ref. [40], the authors prepare the Lanczos states variationally using a cost function similar to (3.3), and then evaluate the matrix elements as

$$\alpha_k = \langle 0 | \hat{U}^\dagger(\boldsymbol{\theta}_k) \hat{H} \hat{U}(\boldsymbol{\theta}_k) | 0 \rangle \quad (\text{A.1})$$

$$\beta_k^2 = \langle 0 | \hat{U}^\dagger(\boldsymbol{\theta}_{k-1}) \hat{H}^2 \hat{U}(\boldsymbol{\theta}_{k-1}) | 0 \rangle - \alpha_{k-1}^2 - \beta_{k-1}^2, \quad (\text{A.2})$$

where $|\chi_k\rangle = \hat{U}(\boldsymbol{\theta}_k) | 0 \rangle$ is the k 'th Lanczos state in the recursion, and $\boldsymbol{\theta}_k$ are variational parameters found by optimizing the cost function (see Eq. 7 in [40]). Assuming uniform allocation of shots

between the Pauli strings in the Hamiltonian, the variance of the estimated expectation value of (A.1) and the first term in (A.2) are

$$\sigma_{\text{lan},\alpha}^2 = \sum_{j=1}^{L'} h_j^2 \frac{1 - \Pi_{k,j}^2}{M_\alpha} \leq \sum_{j=1}^{L'} \frac{h_j^2}{M_\alpha} \quad (\text{A.3})$$

$$\sigma_{\text{lan},\beta}^2 = \sum_{j=1}^Q \tilde{h}_j^2 \frac{1 - \Pi_{k,j}^2}{M_\beta} \leq \sum_{j=1}^Q \frac{\tilde{h}_j^2}{M_\beta} \quad (\text{A.4})$$

where M_α and M_β are the number of measurements, $\Pi_{k,j} = \langle \Psi_k | \hat{P}_j | \Psi_k \rangle$, $L' < L$ where L is the number of terms in the qubit (Jordan-Wigner) Hamiltonian and L' is the number of terms with non-zero variance, and $Q < L'^2$ is the number of terms in \hat{H}^2 with non-zero variance. For example, consider $\hat{H} = h_a \hat{P}_a + h_b \hat{P}_b$ then $\hat{H}^2 = h_a^2 + h_b^2 + h_a h_b (\hat{P}_a \hat{P}_b + \hat{P}_b \hat{P}_a)$ where the terms h_a^2 and h_b^2 do not contribute to the variance and should not be included in the sum (A.4). Further, if $\hat{P}_a \hat{P}_b = -\hat{P}_b \hat{P}_a$ then these terms should be removed as well. The total number of measurements for a N_{it} -iteration Lanczos recursion is therefore

$$M_{\text{lan}}^{\text{tot}} = N_{\text{it}}(L' M_\alpha + Q M_\beta) = N_{\text{it}} \left(L' \sum_{j=1}^{L'} \frac{h_j^2}{\sigma_{\text{lan},\alpha}^2} + Q \sum_{j=1}^Q \frac{\tilde{h}_j^2}{\sigma_{\text{lan},\beta}^2} \right). \quad (\text{A.5})$$

For the Chebyshev method, the variance of the estimated expectation value of the first term in (3.3), i.e., the most expensive term, is

$$\sigma_{\text{che}}^2 = \frac{4 \|\chi_{k-1}\|^2}{\Delta^2} \sum_{j=1}^{L'} h_j^2 \frac{1 - \Pi_{k,j}^2}{M} \leq \frac{4 \|\chi_{k-1}\|^2}{\Delta^2} \sum_{j=1}^{L'} \frac{h_j^2}{M} \quad (\text{A.6})$$

where $\Delta = (E_{\text{max}} - E_{\text{min}})/2$ comes from the scaling of the Hamiltonian in (2.4). The second term in (3.3) and the overlap in (3.4) correspond to a single Pauli string estimation and do not significantly add to the run-time and these contributions are omitted here. Note, the k -iteration dependency on the variance for the chebyshev method due to the normalizing constant. The total number of measurements for a K -term Chebyshev expansion is therefore

$$M_{\text{che}}^{\text{tot}} = L' \sum_{j=1}^{L'} \frac{4 h_j^2}{\Delta^2 \sigma_{\text{che}}^2} \sum_{k=1}^K \|\chi_{k-1}\|^2. \quad (\text{A.7})$$

We compare the Lanczos and the Chebyshev method for computing the spectral function for molecular hydrogen in 6-31G in Fig. 2. For molecular hydrogen in 6-31G we have the following parameters:

$$L' = 184 \tag{A.8}$$

$$Q = 2942 \tag{A.9}$$

$$\sum_{j=1}^{L'} h_j^2 \approx 7 \tag{A.10}$$

$$\sum_{j=1}^Q \tilde{h}_j^2 \approx 206, \tag{A.11}$$

$$\Delta^2 \approx 2.4. \tag{A.12}$$

Here OpenFermion [57] and Psi4 [58] were used to extract the molecular parameters. In Eqs. (A.10) and (A.11) the identity terms in the Jordan-Wigner transformation of the molecular electronic Hamiltonian are removed.

Setting $\sigma_{\text{lan},\alpha}^2 = \sigma_{\text{lan},\beta}^2 = \sigma_{\text{che}}^2 = 10^{-n}$ with $n \in \mathbb{Z}^+$, the total number of measurements are approximately

$$M_{\text{lan}}^{\text{tot}} = 607.349 \cdot N_{\text{it}} \cdot 10^n \tag{A.13}$$

$$M_{\text{che}}^{\text{tot}} = 2147 \cdot 10^n \sum_{k=1}^K |||\chi_{k-1}\rangle||^2 \tag{A.14}$$

$$\frac{M_{\text{che}}^{\text{tot}}}{M_{\text{lan}}^{\text{tot}}} = \frac{3.53}{10^3 N_{\text{it}}} \sum_{k=1}^K |||\chi_{k-1}\rangle||^2. \tag{A.15}$$

For the electron affinity and ionization potential in Fig. 2, the number of Lanczos iterations are about $N_{\text{it}} = 10$ and $N_{\text{it}} = 2$, respectively, since there are about ten and two poles in the spectrum. We find that setting $K = 70.000$ then $\sum_{k=1}^K |||\chi_{k-1}\rangle||^2 = 505$ which is still less than $\frac{10^3 N_{\text{it}}}{3.53}$ for $N_{\text{it}} = 2$. In the simulations we set $K = 40.000$, which is large enough to reduce the background oscillation, resulting in a lower run-time than the Lanczos method.

[1] J. Lee, D. W. Berry, C. Gidney, W. J. Huggins, J. R. McClean, N. Wiebe, and R. Babbush, [PRX Quantum](#) **2**, 030305 (2021).

- [2] Y. Su, D. W. Berry, N. Wiebe, N. Rubin, and R. Babbush, [PRX Quantum **2**, 040332 \(2021\)](#).
- [3] N. P. Bauman, H. Liu, E. J. Bylaska, S. Krishnamoorthy, G. H. Low, C. E. Granade, N. Wiebe, N. A. Baker, B. Peng, M. Roetteler, M. Troyer, and K. Kowalski, [Journal of Chemical Theory and Computation **17**, 201 \(2021\)](#).
- [4] P. W. K. Jensen, L. B. Kristensen, J. S. Kottmann, and A. Aspuru-Guzik, [Quantum Science and Technology **6**, 015004 \(2020\)](#).
- [5] T. E. O'Brien, M. Streif, N. C. Rubin, R. Santagati, Y. Su, W. J. Huggins, J. J. Goings, N. Moll, E. Kyoseva, M. Degroote, C. S. Tautermann, J. Lee, D. W. Berry, N. Wiebe, and R. Babbush, [arXiv **10.48550/arXiv.2111.12437** \(2021\)](#).
- [6] J. R. McClean, J. Romero, R. Babbush, and A. Aspuru-Guzik, [New Journal of Physics **18**, 023023 \(2016\)](#).
- [7] A. Peruzzo, J. McClean, P. Shadbolt, M.-H. Yung, X.-Q. Zhou, P. J. Love, A. Aspuru-Guzik, and J. L. O'Brien, [Nature Communications **5**, 4213 \(2014\)](#).
- [8] O. Higgott, D. Wang, and S. Brierley, [Quantum **3**, 156 \(2019\)](#).
- [9] I. G. Ryabinkin, S. N. Genin, and A. F. Izmaylov, [Journal of Chemical Theory and Computation **15**, 249 \(2019\)](#).
- [10] T.-C. Yen, R. A. Lang, and A. F. Izmaylov, [The Journal of Chemical Physics **151**, 164111 \(2019\)](#).
- [11] J. R. McClean, M. E. Schwartz, J. Carter, and W. A. de Jong, [Physical Review A **95**, 042308 \(2017\)](#).
- [12] P. J. Ollitrault, A. Kandala, C.-F. Chen, P. K. Barkoutsos, A. Mezzacapo, M. Pistoia, S. Sheldon, S. Woerner, J. Gambetta, and I. Tavernelli, [Physical Review Research **2**, 043140 \(2020\)](#).
- [13] T. E. O'Brien, B. Senjean, R. Sagastizabal, X. Bonet-Monroig, A. Dutkiewicz, F. Buda, L. DiCarlo, and L. Visscher, [npj Quantum Information **5**, 1 \(2019\)](#).
- [14] K. Mitarai, Y. O. Nakagawa, and W. Mizukami, [Physical Review Research **2**, 013129 \(2020\)](#).
- [15] J. F. Gonthier, M. D. Radin, C. Buda, E. J. Daskocil, C. M. Abuan, and J. Romero, [arXiv **10.48550/arxiv.2012.04001** \(2020\)](#).
- [16] R. McWeeny, *Methods of molecular quantum mechanics*, 2nd ed., Theoretical chemistry (Academic Press, London, 1992).
- [17] A. L. Fetter, J. D. Walecka, and Physics, *Quantum Theory of Many-Particle Systems (Dover Books on Physics)* (Dover Publications, 2003) p. 640.
- [18] J. Schirmer, *Many-Body Methods for Atoms, Molecules and Clusters*, Lecture Notes in Chemistry, Vol. 94 (Springer International Publishing, Cham, 2018).

- [19] Y. Tong, D. An, N. Wiebe, and L. Lin, [Physical Review A **104**, 032422 \(2021\)](#).
- [20] X. Cai, W.-H. Fang, H. Fan, and Z. Li, [Physical Review Research **2**, 033324 \(2020\)](#).
- [21] T. Keen, E. Dumitrescu, and Y. Wang, [arXiv **10.48550/arxiv.2112.05731** \(2021\)](#).
- [22] T. Kosugi and Y.-i. Matsushita, [Physical Review A **101**, 012330 \(2020\)](#).
- [23] X. Yuan, S. Endo, Q. Zhao, Y. Li, and S. Benjamin, [Quantum **3**, 191 \(2019\)](#).
- [24] M. Motta, C. Sun, A. T. K. Tan, M. J. O. Rourke, E. Ye, A. J. Minnich, F. G. S. L. Brandao, and G. K.-L. Chan, [Nature Physics **16**, 205 \(2020\)](#).
- [25] S. Endo, I. Kurata, and Y. O. Nakagawa, [Physical Review Research **2**, 033281 \(2020\)](#).
- [26] S.-N. Sun, M. Motta, R. N. Tazhigulov, A. T. K. Tan, G. K.-L. Chan, and A. J. Minnich, [PRX Quantum **2**, 010317 \(2021\)](#).
- [27] R. N. Tazhigulov, S.-N. Sun, R. Haghshenas, H. Zhai, A. T. K. Tan, N. C. Rubin, R. Babbush, A. J. Minnich, and G. K.-L. Chan, [arXiv **10.48550/arXiv.2203.15291** \(2022\)](#).
- [28] R. Sakurai, W. Mizukami, and H. Shinaoka, [arXiv **10.48550/arXiv.2112.02764** \(2021\)](#).
- [29] H. Chen, M. Nusspickel, J. Tilly, and G. H. Booth, [Physical Review A **104**, 032405 \(2021\)](#).
- [30] J. Rizzo, F. Libbi, F. Tacchino, P. J. Ollitrault, N. Marzari, and I. Tavernelli, [arXiv **10.48550/arXiv.2201.01826** \(2022\)](#).
- [31] J. Zhu, Y. O. Nakagawa, C.-F. Li, G.-C. Guo, and Y.-S. Zhang, [arXiv **10.48550/arXiv.2104.12361** \(2021\)](#).
- [32] K. Huang, X. Cai, H. Li, Z.-Y. Ge, R. Hou, H. Li, T. Liu, Y. Shi, C. Chen, D. Zheng, K. Xu, Z.-B. Liu, Z. Li, H. Fan, and W.-H. Fang, [arXiv **10.48550/arXiv.2201.02426** \(2022\)](#).
- [33] T. Keen, T. Maier, S. Johnston, and P. Lougovski, [Quantum Science and Technology **5**, 035001 \(2020\)](#).
- [34] A. Weisse, G. Wellein, A. Alvermann, and H. Fehske, [Reviews of Modern Physics **78**, 275 \(2006\)](#).
- [35] A. Ferreira and E. R. Mucciolo, [Physical Review Letters **115**, 106601 \(2015\)](#).
- [36] J. E. Sobczyk and A. Roggero, [arXiv **10.48550/arXiv.2110.02108** \(2021\)](#).
- [37] P. Rall, [Physical Review A **102**, 022408 \(2020\)](#).
- [38] H. Wang, J. Nan, X. Qiu, and X. Li, [arXiv **10.48550/arXiv.2202.01170** \(2022\)](#).
- [39] T. E. Baker, [Physical Review A **103**, 032404 \(2021\)](#).
- [40] F. Jamet, A. Agarwal, C. Lupo, D. E. Browne, C. Weber, and I. Rungger, [arXiv **10.48550/arXiv.2105.13298** \(2021\)](#).
- [41] T. Rivlin, [Chebyshev Polynomials: From Approximation Theory to Algebra and Number Theory](#):

Second Edition, Dover Books on Mathematics (Courier Dover Publications, 2020).

- [42] R. Chen and H. Guo, [The Journal of Chemical Physics](#) **105**, 3569 (1996).
- [43] R. Chen and H. Guo, [Computer Physics Communications](#) **119**, 19 (1999).
- [44] H. Tal-Ezer and R. Kosloff, [The Journal of Chemical Physics](#) **81**, 3967 (1984).
- [45] W. Zhu, Y. Huang, D. Kouri, C. Chandler, and D. K. Hoffman, [Chemical Physics Letters](#) **217**, 73 (1994).
- [46] R. Chen and H. Guo, [The Journal of Chemical Physics](#) **108**, 6068 (1998).
- [47] R. Kosloff and H. Tal-Ezer, [Chemical Physics Letters](#) **127**, 223 (1986).
- [48] C. Lanczos, [Journal of Research of the National Bureau of Standards](#) **45**, 255 (1950).
- [49] T. Helgaker, P. Joergensen, and J. Olsen, *Molecular Electronic-Structure Theory* (John Wiley & Sons, Ltd, Chichester, UK, 2000).
- [50] J. Olsen, B. O. Roos, P. Joergensen, and H. J. A. Jensen, [The Journal of Chemical Physics](#) **89**, 2185 (1988).
- [51] W. Duch, *GRMS or Graphical Representation of Model Spaces*, edited by G. Berthier, M. J. S. Dewar, H. Fischer, K. Fukui, G. G. Hall, J. Hinze, H. H. Jaffé, J. Jortner, W. Kutzelnigg, K. Ruedenberg, and J. Tomasi, Lecture Notes in Chemistry, Vol. 42 (Springer Berlin Heidelberg, Berlin, Heidelberg, 1986).
- [52] B. O’Gorman, S. Irani, J. Whitfield, and B. Fefferman, arXiv [10.48550/arXiv.2103.08215](#) (2021).
- [53] A. Anand, P. Schleich, S. Alperin-Lea, P. W. K. Jensen, S. Sim, M. Diaz-Tinoco, J. S. Kottmann, M. Degroote, A. F. Izmaylov, and A. Aspuru-Guzik, [Chemical Society Reviews](#) , 10.1039.D1CS00932J (2022).
- [54] Y. Cao, J. Romero, J. P. Olson, M. Degroote, P. D. Johnson, M. Kieferova, I. D. Kivlichan, T. Menke, B. Peropadre, N. P. D. Sawaya, S. Sim, L. Veis, and A. Aspuru-Guzik, [Chemical Reviews](#) **119**, 10856 (2019).
- [55] Y. Meir and N. S. Wingreen, [Physical Review Letters](#) **68**, 2512 (1992).
- [56] J. Oddershede, P. Joergensen, and D. L. Yeager, [Computer Physics Reports](#) **2**, 33 (1984).
- [57] J. R. McClean, N. C. Rubin, K. J. Sung, I. D. Kivlichan, X. Bonet-Monroig, Y. Cao, C. Dai, E. S. Fried, C. Gidney, B. Gimby, P. Gokhale, T. Häner, T. Hardikar, V. Havlíček, O. Higgott, C. Huang, J. Izaac, Z. Jiang, X. Liu, S. McArdle, M. Neeley, T. O’Brien, B. O’Gorman, I. Ozfidan, M. D. Radin, J. Romero, N. P. D. Sawaya, B. Senjean, K. Setia, S. Sim, D. S. Steiger, M. Steudtner, Q. Sun, W. Sun, D. Wang, F. Zhang, and R. Babbush, [Quantum Science and Technology](#) **5**, 034014

(2020).

- [58] J. M. Turney, A. C. Simmonett, R. M. Parrish, E. G. Hohenstein, F. A. Evangelista, J. T. Fermann, B. J. Mintz, L. A. Burns, J. J. Wilke, M. L. Abrams, N. J. Russ, M. L. Leininger, C. L. Janssen, E. T. Seidl, W. D. Allen, H. F. Schaefer, R. A. King, E. F. Valeev, C. D. Sherrill, and T. D. Crawford, *WIREs Computational Molecular Science* **2**, 556 (2012).
- [59] Y. Huang, W. Zhu, D. J. Kouri, and D. K. Hoffman, *Chemical Physics Letters* **206**, 96 (1993).
- [60] H. Guo, in *Reviews in Computational Chemistry*, edited by K. B. Lipkowitz and T. R. Cundari (John Wiley & Sons, Inc., Hoboken, NJ, USA, 2007) pp. 285–348.
- [61] E. Pavarini, E. Koch, D. Vollhardt, A. I. Lichtenstein, I. for Advanced Simulation, G. R. S. for Simulation Sciences, and D. Forschungsgemeinschaft, eds., *The LDA+DMFT approach to strongly correlated materials: lecture notes of the Autumn School 2011 Hands-on LDA+DMFT: at Forschungszentrum Jülich, 4-7 October 2011*, Schriften des Forschungszentrums Jülich. Reihe Modeling and Simulation No. Band 1 (Forschungszentrum Jülich, Zentralbibliothek, Verl, Jülich, 2011) meeting Name: Autumn School Hands-on LDA+DMFT.
- [62] F. Kuhnert, *ZAMM - Zeitschrift für Angewandte Mathematik und Mechanik* **61**, 345 (1981).
- [63] C. C. Paige, *IMA Journal of Applied Mathematics* **18**, 341 (1976).
- [64] C. C. Paige, *IMA Journal of Applied Mathematics* **10**, 373 (1972).
- [65] C. Paige, *Linear Algebra and its Applications* **34**, 235 (1980).
- [66] J. Cullum and R. A. Willoughby, *Journal of Computational and Applied Mathematics* **12-13**, 37 (1985).
- [67] D. W. Berry, A. M. Childs, and R. Kothari, in *2015 IEEE 56th Annual Symposium on Foundations of Computer Science* (IEEE, Berkeley, CA, USA, 2015) pp. 792–809.
- [68] G. H. Low and I. L. Chuang, *Physical Review Letters* **118**, 010501 (2017).
- [69] S. Barison, F. Vicentini, and G. Carleo, *Quantum* **5**, 512 (2021).
- [70] J. R. McClean, S. Boixo, V. N. Smelyanskiy, R. Babbush, and H. Neven, *Nature Communications* **9**, 4812 (2018).
- [71] H. R. Grimsley, G. S. Barron, E. Barnes, S. E. Economou, and N. J. Mayhall, arXiv [10.48550/arXiv.2204.07179](https://arxiv.org/abs/10.48550/arXiv.2204.07179) (2022).
- [72] Y. Dong, L. Lin, and Y. Tong, arXiv <https://arxiv.org/abs/2204.05955> (2022).
- [73] M. Irfan, S. R. Kuppuswamy, D. Varjas, P. M. Perez-Piskunow, R. Skolasinski, M. Wimmer, and A. R. Akhmerov, arXiv [10.48550/arXiv.1909.09649](https://arxiv.org/abs/10.48550/arXiv.1909.09649) (2019).

- [74] G. H. Booth and G. K.-L. Chan, [Physical Review B](#) **91**, 155107 (2015).